



nanoFIS 2016

# Schottky diode formation in GaAs nanowires by heterogeneous contact deposition

Suzanne Lancaster<sup>a,\*</sup>, Aaron Maxwell Andrews<sup>a</sup>, Tobias Zederbauer<sup>a</sup>,  
Donald MacFarland<sup>a</sup>, Gottfried Strasser<sup>a</sup>, Hermann Detz<sup>a,b</sup>

<sup>a</sup>Center for Micro- and Nanostructures, Institute for Solid State Electronics, TU Wien, 1040 Vienna, Austria

<sup>b</sup>Austrian Academy of Sciences, 1010 Vienna, Austria

---

## Abstract

III-V semiconductor nanowires (NWs) have many potential applications in future optoelectronic devices. Here we present a simple method to create single-nanowire and array Schottky diodes in undoped and Si-doped GaAs nanowires using one p- and one n-type electrical contact, and we investigate the transport properties of these nanodevices. The devices showed on/off ratios up to  $10^5$ , making them suitable for a wide range of potential applications such as photodetectors or Schottky barrier field effect transistors.

© 2017 The Authors. Published by Elsevier Ltd. This is an open access article under the CC BY-NC-ND license (<http://creativecommons.org/licenses/by-nc-nd/4.0/>).

Selection and/or Peer-review under responsibility of nanoFIS 2016 – Functional Integrated nano Systems.

*Keywords:* nanowires; diodes; nanowire electronics; nanowire arrays; Schottky barriers; nanocontacts; contact printing; E-beam lithography

---

## 1. Introduction

GaAs nanowires (NWs) are attractive candidates for nanoscale semiconductor devices, particularly in optoelectronics, for a variety of reasons; their one-dimensionality allows a more flexible choice of material combinations in heterostructures due to a relaxation of strain in lattice-mismatched materials [1] and facilitates the integration of III-V materials on silicon [2, 3], their large aspect ratios lead to confinement and often interesting

---

\* Corresponding author. Tel.: +43 (1) 58801 – 362 15.

E-mail address: [Suzanne.lancaster@tuwien.ac.at](mailto:Suzanne.lancaster@tuwien.ac.at)

absorption and emission effects [4, 5] and in certain applications such as photovoltaics, nanowire devices have been proven more efficient than planar devices [6].

To this end, much research has been conducted on III-V nanowires, with one of the biggest challenges remaining the formation of good electrical contacts, particularly to single-wire devices. Often contacts with the same metallization will exhibit either Ohmic or rectifying behaviour, even when deposited on wires from the same sample [7, 8]. This can be due to subtle changes in the contact properties [9], a native oxide layer between the nanowire and contact [10], or local differences in the structure and composition of the nanowire itself. This makes reproducibility of nanowire devices difficult and hinders progress in device development.

Using undoped and p-doped nanowires, by depositing one p- and one n-type contact, we aimed to create Schottky diode structures with high on-off current ratios purely by contact engineering. Potential applications range from Schottky barrier transistors [11], to sensors [12], to nanowire photodetectors [13, 14] which could exploit the polarization selectivity of nanowires [15].

## 2. Growth and processing

All GaAs nanowires described here were grown by solid-source molecular beam epitaxy (MBE) using the self-catalyzed vapor-liquid-solid (VLS) method [16, 17]. The native oxide of Si (111) substrates was used for the nucleation of the Ga droplets. Nanowire growth was performed at a substrate temperature of 630 °C under  $\text{As}_4$  limited conditions at typical equivalent layer growth rates of 0.1  $\mu\text{m}/\text{h}$  for Ga. For doping, a Si effusion cell was operated for an equivalent doping of  $1.75 \times 10^{18} / \text{cm}^3$  for a GaAs growth rate of 1  $\mu\text{m}/\text{h}$ . After growth, the samples were cooled under residual  $\text{As}_4$  flux. Wires were suspended in isopropanol and dispersed onto a p-doped Si substrate with 100nm thermal oxide, pre-patterned with Ti/Au contact pads. Typical undoped nanowire dimensions after dispersion, as measured from SEM images, were a length of  $5.66 \pm 0.26 \mu\text{m}$  and a diameter of  $92.5 \pm 7.5 \text{ nm}$ . For doped wires the values were  $2.70 \pm 0.31 \mu\text{m}$  for wire length and  $60.3 \pm 6.5 \text{ nm}$  for wire diameter. Some discrepancy in wire length was expected due to the dispersion technique.

Four types of heterogeneously contacted nanowire device were processed: single-wire devices based on undoped or Si-doped GaAs nanowires, and array devices based on multiple horizontally dispersed undoped or Si-doped nanowires. First, single-wire devices were fabricated. Individual wires were identified and contacted via e-beam lithography (EBL) in a multistep process. One set of contacts was defined and contacted with Au/Zn/Au (5/10/100nm) in a thermal evaporation system. After lift-off, the samples were reloaded into the EBL system to define second contacts, after which Ge/Au/Ni/Au (10/20/10/60nm) was deposited in an e-beam evaporation system. Before each metal evaporation, the native oxide from the GaAs wires was removed by a 1:1 HCl:H<sub>2</sub>O etch for 10s. A schematic and SEM image of the final device are shown in figure 1. Since GaAs nanowires doped with silicon are expected to be p-type [18], Au/Zn/Au should form an Ohmic contact to the wire, while the Ge/Au/Ni/Au should create a Schottky barrier.

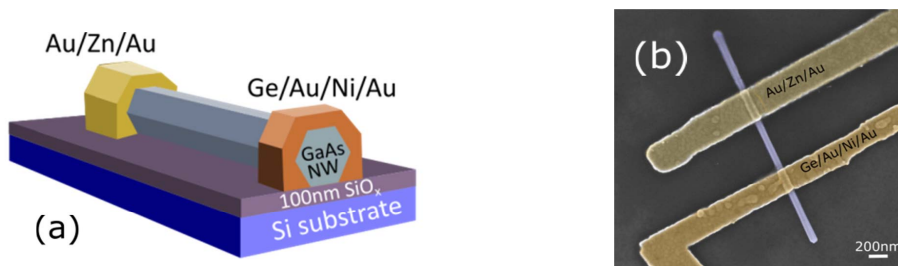


Fig. 1: (a) Schematic of single-wire device with heterogeneous contacts; (b) SEM image of a fabricated GaAs-nanowire-based Schottky diode device.. The nanowire is first dispersed on the SiO<sub>x</sub> substrate from an isopropanol solution. Subsequently, p- and n-type contacts are fabricated by electron-beam lithography, evaporation and lift-off steps.

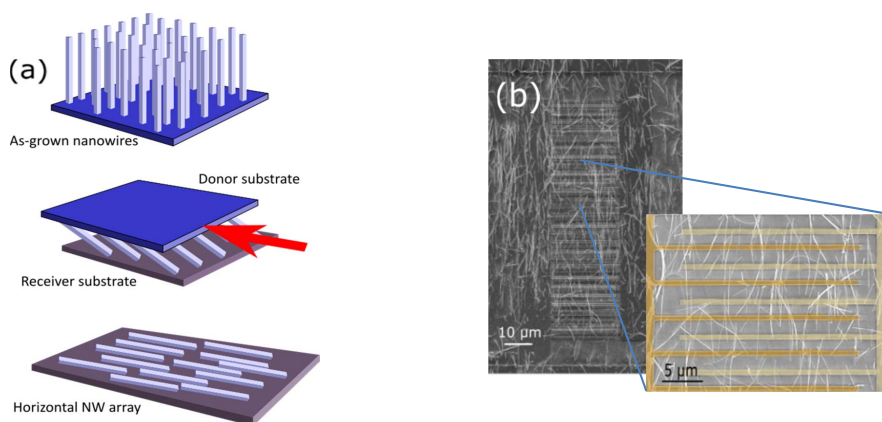


Fig. 2: (a) Contact printing method used to create ordered horizontal nanowire arrays; (b) SEM images of an array-based Schottky diode device, showing well-aligned nanowires, including a close-up view of the heterogeneous contact geometry.

These devices were then replicated on arrays of dispersed nanowires. This allows the benefits of individual nanowires to be maintained, whilst allowing for higher current densities due to the higher number of conducting channels. With these devices there is an added controllable parameter, as the density of wires on the growth substrate affects the density of wires in the end device, and could be reliably determined by using ordered arrays of nanowires, which provide well-controlled densities and uniformity [19].

Arrays were formed with a similar method to single-wire devices, but with a contact printing method (fig. 2a) used to transfer the wires with high density and preferential orientation. During each patterning step a series of contacting ‘fingers’ was defined, leading to an array of alternating p- and n-type contacts (fig. 2b).

### 3. Results

Electrical measurements were carried out in a Keithley 4200 semiconductor probe station. 4-pt measurements with homogeneous Au/Zn/Au contacts revealed a resistivity of  $3.56 \Omega\text{cm}$  for p-doped wires, and using the method described in ref. [4], a doping density of around  $1 \times 10^{17} \text{cm}^{-3}$  was calculated. Similar measurements on undoped wires were unsuccessful when contacted homogeneously with either Au/Zn/Au or Ge/Au/Ni/Au, indicating negligible background doping.

When heterogeneous contacts were deposited, undoped single-wire devices were conductive, showing back-to-back Schottky characteristics (fig. 3a). Doped devices showed clear single-rectifying behavior (fig. 3b) indicative of a Schottky diode, which was reproducible across devices.

For doped devices this rectifying behavior displays on/off ratios of up to  $10^5$ . However, when compared to planar GaAs Schottky diodes, the reverse current is still significant. This has been attributed in such nano-Schottky devices to a non-negligible tunneling current at the contacts [20]. From figure 3 we can see that the photoresponsivity (measured under tungsten lamp illumination) is highest in this reverse tunneling current.

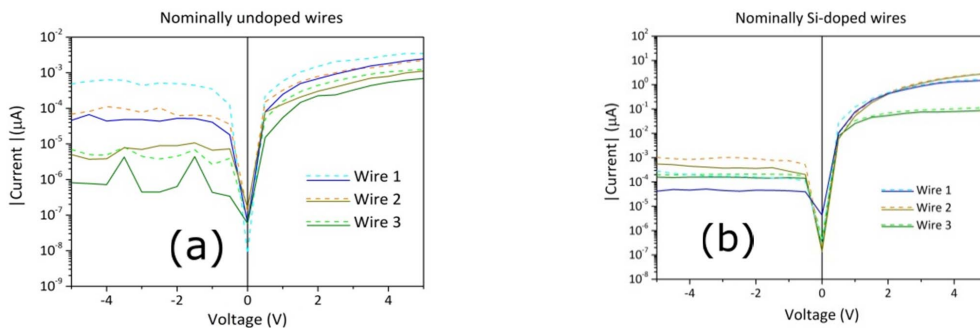


Fig. 3: IV measurements of heterogeneously contacted (a) undoped and (b) p-doped GaAs nanowires. Dashed lines indicate current under tungsten lamp illumination. All measurements were performed at room temperature.

For arrays of nanowires (fig.4), the forward current was seen to scale with the number of wires in a device. Forward currents up to 15μA at 5V forward bias were achieved for doped array devices with approximately 30 nanowires, which is a factor of 10 higher than for a single-wire device. This does however suggest that some wires in the array are not fully contributing to the device, possibly due to poor contact or defects in the wires. These parasitic wires could contribute to the large increase in the reverse current, thus reducing the device on/off ratio, and would need to be addressed in future devices by optimizing either the wire placement or the contact deposition technique.

The behavior of a non-ideal diode is given by the equation [21]:

$$I = I_0(e^{q(V-V_{th})/nkT} - 1), \tag{1}$$

Where q, V, k and T have their usual meanings,  $V_{th}$  is the threshold voltage, n is the ideality factor of the diode, and  $I_0$  is the saturation current, given by:

$$I_0 = AA^*T^2 e^{(-q\phi_B/kT)}, \tag{2}$$

Where A is the cross-sectional area of the diode,  $A^*$  is the material’s Richardson constant (the value of  $1.5e4$  [22] is used here), and  $\phi_B$  is the Schottky barrier height.

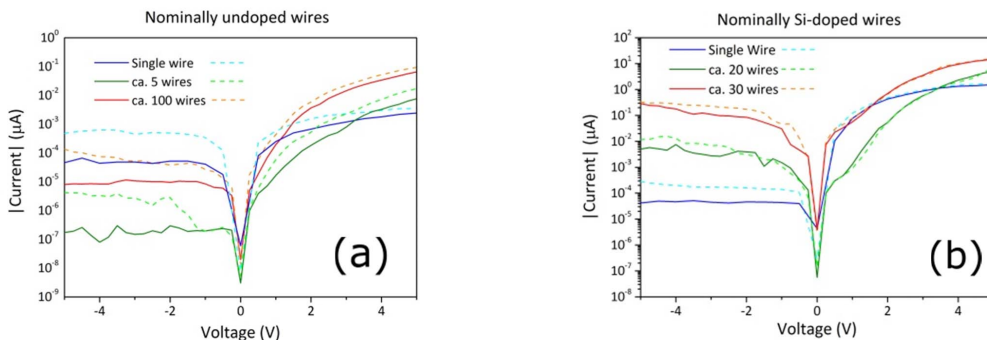


Fig. 4: Current-Voltage measurements on arrays of heterogeneously contacted (a) undoped and (b) p-doped nanowires, with different numbers of nanowires per device. Dashed lines indicate current under tungsten lamp illumination.

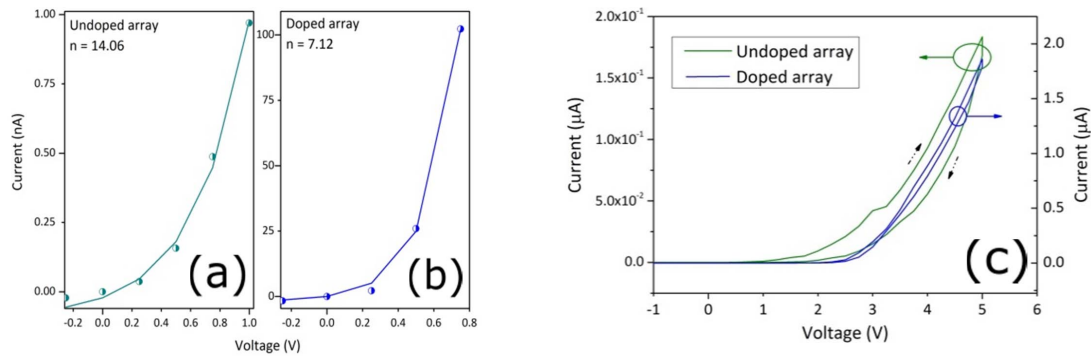


Fig. 5: Experimental (dots) and fitted (line) data for (a) undoped and (b) doped array devices; (c) IV hysteresis curves for doped and undoped nanowire arrays. Dashed arrows indicate direction of voltage sweep.

Fitting our IV curves at forward bias to equation 1 allows us to calculate the ideality factor. These fits are plotted for undoped and doped array devices in figures 5a & b. The ideality factors calculated for two typical devices were 14 for an undoped array and 7.1 for a doped array, thus deviating from the expected value of 1 for an ideal diode. This large deviation has been seen in Schottky diodes on GaN nanowires [23] with ideality factors of up to 17.8 at room temperature, and can be attributed to several factors. Firstly, a tunneling current at the contact, as mentioned earlier, would modify the diode characteristics and give a high ideality factor [24]. Secondly, while the nanowire native oxide should be removed in the pre-processing, there may still be an oxide layer at the wire-contact interface, which for nanocontacts can have an impact even at small thicknesses. This is evidenced particularly for undoped devices in the hysteresis curves (fig. 5c), where a large hysteresis indicates charging at the contacts, which could be attributed to an interfacial oxide layer [25].

#### 4. Conclusion

We have demonstrated Schottky behavior in undoped and p-doped nanowires, by using a p-type Au/Zn/Au and n-type Ge/Au/Ni/Au contact. For undoped nanowires, devices show a high photoresponsivity, particularly in reverse bias, which could be exploited in photodetectors. Si-doped nanowire devices show Schottky diode behavior with high on-off currents, and could form the basis of Schottky barrier FETs and phototransistors.

We also investigated possible scaling of such devices by using contact-printed horizontal arrays of nanowires. Again, the arrays exhibited single-rectifying Schottky diode behavior, and as such arrays could be used for scaling-up of nanowire devices. The current through the device could be directly controlled via the number of electrically active nanowires in an array. Since the wires are grown directly onto silicon substrates, it should be possible to recreate these Schottky arrays on as-grown nanowire arrays, allowing for integration in vertical nanowire devices.

Finally, the ideality factors for such array devices were calculated. The ideality factors, ranging from 7 to 14 for doped/undoped devices respectively, deviated from the expected value of 1, which was attributed to tunneling in the devices and an interfacial layer between nanowire and contact. Nevertheless, devices fabricated with the process described repeatedly showed single-rectifying behavior, indicating that the technique can be used as a basis for many applications.

#### Acknowledgements

The authors would like to thank the Austrian Science Fund (FWF): P26100-N27 (H2N) for funding. HD acknowledges financial support through an APART fellowship from the Austrian Academy of Sciences.

## References

- [1] P. Caroff, J.B. Wagner, K.A. Dick, H.A. Nilsson, M. Jeppsson, K. Deppert, L. Samuelson, L.R. Wallenberg, L-E Wernersson. *Small*, 2008, **4**(7), 878-882.
- [2] T. Mårtensson, C.P.T. Svensson, B.A. Wacaser, M.W. Larsson, W. Seifert, K. Deppert, A. Gustafsson, L.R. Wallenberg, and L. Samuelson. *Nano Lett.*, 2004, **4**(10), 1987-1990.
- [3] A. Brenneis, J. Overbeck, J. Treu, S. Hertenberger, S. Morkötter, M. Döblinger, J.J. Finley, G. Abstreiter, G. Koblmüller, A.W. Holleitner, 2015, *ACS nano*, **9**(10), pp.9849-9858.
- [4] X. Duan, J. Wang, C.M. Lieber. *Appl. Phys. Lett.*, 2000, **76**(9), 1116-1118.
- [5] M. N. Makhonin, A. P. Foster, A. B. Krysa, P. W. Fry, D. G. Davies, T. Grange, T. Walther, M. S. Skolnick, L. R. Wilson. *Nano lett.*, 2013, **13**(3) 861-865.
- [6] J. Kupec, R.L. Stoop, B.Witzigmann, *Opt. Express*, 2010, **18**(26), 27589-27605
- [7] Z. Zhang, K. Yao, Y. Liu, C. Jin, X. Liang, Q. Chen, and L-M. Peng. *Adv. Func. Mat.*, 2007, **17**(14), 2478-2489.
- [8] Y-F. Lin, W-B. Jian. *Nano lett.*, 2008, **8**(10), 3146-3150.
- [9] F. Léonard, A.A. Talin. *Nat. nanotech.* 2011, **6**(12), 773-783.
- [10] M. J. L.Sourribes, I. Isakov, M. Panfilova, P. A. Warburton. *Nanotechnology*, 2013, **24**(4), 045703.
- [11] S. Pregl, W.M. Weber, D. Nozaki, J. Kunstmann, L. Baraban, J. Opitz, T. Mikolajick, G. Cuniberti. *Nano Research*, 2013, **6**(6), 381-388.
- [12] Z. Fan, D. Wang, P-C. Chang, W-Y. Tseng, J.G. Lu. *Appl. Phys. Lett.*, 2004, **85**(24 ), 5923-5925.
- [13] E.M. Gallo, G. Chen, M. Currie, T. McGuckin, P. Prete, N. Lovergine, B. Nabet, J.E. Spanier. *Appl. Phys. Lett.*. 2011, **98**(24), 241113.
- [14] H.Wang, *Appl. Phys. Lett.*, 2013, **103**(9), 093101.
- [15] I. Zardo, S. Conesa-Boj, F. Peiro, J. R. Morante, J. Arbiol, E. Uccelli, G. Abstreiter, A. Fontcuberta i Morral. *Phys. Rev. B* 2009 **80**(24), 245324.
- [16] A. Fontcuberta i Morral, C. Colombo, G. Abstreiter, J. Arbiol, J. R. Morante. *Appl. Phys. Lett.*, 2008, **92**(6), 063112.
- [17] F. Bastiman, H. Küpers, C. Somaschini, L. Geelhaar. *Nanotechnology*, 2016, **27**(9) ,095601.
- [18] J. Dufouleur, C. Colombo, T. Garma, B. Ketterer, E. Uccelli, M. Nicotra, A. Fontcuberta i Morral. *Nano lett.*, 2010, **10**(5), 1734-1740.
- [19] S. Plissard, G. Larrieu, X. Wallart, P. Caroff. *Nanotechnology*, 2011, **22**(27), 275602.
- [20] Z. Y. Zhang, C. H. Jin, X. L. Liang, Q. Chen, L-M. Peng. *Appl. Phys. Lett.*, 2006 **88**(7), 073102.
- [21] S. M. Sze, *Physics of Semiconductor Devices*, 3rd Edn. Wiley, New York 2007, p.119.
- [22] M. Missous, E. H. Rhoderick, D. A. Woolf, S. P. Wilkes. *Semiconductor science and technology*, 1992, **7**(2)218.
- [23] J.R. Kim, H. Oh, H. M. So, J-J. Kim, J. Kim, C.J. Lee, and S.C. Lyu. *Nanotechnology*, 2002, **13**(5), 701
- [24] S-Y. Lee, and S-K. Lee. *Nanotechnology*, 2007, **18**(49), 495701.
- [25] J.B. Yang, T.C. Chang, J.J. Huang, S.C. Chen, P-C. Yang, Y-T. Chen, H-C. Tseng, S.M. Sze, A-K. Chu, M-J. Tsai, *Thin Solid Films*, 2013, **529**, pp.200-204.